

# Fabrication of non-biofouling polyethylene glycol micro- and nanochannels by ultraviolet-assisted irreversible sealing†

Pilnam Kim,<sup>a</sup> Hoon Eui Jeong,<sup>a</sup> Ali Khademhosseini<sup>b</sup> and Kahp Y. Suh<sup>\*a</sup>

Received 21st July 2006, Accepted 29th August 2006

First published as an Advance Article on the web 14th September 2006

DOI: 10.1039/b610503c

We present a simple and widely applicable method to fabricate micro- and nanochannels comprised entirely of crosslinked polyethylene glycol (PEG) by using UV-assisted irreversible sealing to bond partially crosslinked PEG surfaces. The method developed here can be used to form channels as small as ~50 nm in diameter without using a sophisticated experimental setup. The manufactured channel is a homogeneous conduit made completely from non-biofouling PEG, exhibits robust sealing with minimal swelling and can be used without additional surface modification chemistries, thus significantly enhancing reliability and durability of microfluidic devices. Furthermore, we demonstrate simple analytical assays using PEG microchannels combined with patterned arrays of supported lipid bilayers (SLBs) to detect ligand (biotin)–receptor (streptavidin) interactions.

## Introduction

Microfluidic systems have served as important platforms for cell-based sensing,<sup>1</sup> biochemical analysis,<sup>2,3</sup> and biological analysis<sup>4,5</sup> because they offer miniaturized systems, flexibility of fabrication, reduced use of reagents, reduced production of wastes, increased speed of analysis, and portability.<sup>6</sup> In particular, silicon or glass-based microfluidic devices have been extensively employed as an analytical tool or an implantable microsystem.<sup>7</sup> However these surfaces result in non-specific adsorption of reagent/sample molecules from the surrounding fluid (so called “biofouling”), which is not desired for biological assays and dilute samples. In addition, intrinsic stiffness and the need for expensive clean room facilities has limited the widespread use of silicon and glass devices.<sup>8</sup>

To overcome some of the above-mentioned limitations, poly(dimethylsiloxane) (PDMS) is widely used to fabricate microfluidic channels because of its favorable mechanical/optical properties<sup>9</sup> and its simple manufacturing by rapid prototyping.<sup>10</sup> However, the ability to prevent biofouling and subsequent malfunction of the device is still limited by hydrophobic interactions between PDMS surface and biological samples.<sup>11</sup> When small sample quantities, such as rare proteins are involved, any loss of sample through the system may result in critical error in the final analysis. To solve this challenge, silicon-based (*e.g.*, silicon, glass, quartz, and PDMS) platforms have been surface modified by non-biofouling

materials such as polyethylene glycol (PEG).<sup>10,12–17</sup> It is believed that the resistant nature of PEG-based polymer may be attributed to polymer chain mobility and sterical stabilization force.<sup>18</sup> Surface modification of silicon-based devices with PEG can be performed by physical adsorption,<sup>12</sup> covalent immobilization such as grafting and chemical coupling,<sup>13–15</sup> or gas phase treatment (plasma or deposition).<sup>10,16,17</sup> These efforts have proved successful but may not be able to guarantee conformal coating and long-term stability, *i.e.*, modified PDMS surfaces slowly recover their original hydrophobicity.<sup>19</sup> In addition to PDMS channels, other microfluidic devices have been introduced using different channel materials such as photocurable perfluoropolyethers, biodegradable polymers, photosensitive polymers, and polymerized hydrogels.<sup>20–28</sup> However, biofouling, weak mechanical properties and the need for extensive expertise potentially limit the versatile use of these devices.

Here, we present a simple and widely applicable method to fabricate micro- and nanochannels comprised entirely of crosslinked PEG by using UV-assisted irreversible sealing to bond partially crosslinked PEG surfaces. While photolithography has been used to create PEG microchannels,<sup>29</sup> the method developed here can be used to form channels as small as ~50 nm in diameter without using a sophisticated experimental setup. In addition, to enable the use of PEG, we minimize the swelling of the crosslinked PEG network by adhering the mold to a supporting layer such as a PET [poly(ethylene terephthalate)] film and by increasing its cross-linking density. The resulting channel is a homogeneous conduit made completely from non-biofouling PEG that can be fabricated in a single bonding step, offering potential advantages over previously reported methods that combine bonding and subsequent etching.<sup>20–28</sup> The resulting PEG channels exhibit robust sealing with minimal swelling and can be used without additional surface modification chemistries, thus significantly enhancing reliability and durability of microfluidic devices.

<sup>a</sup>School of Mechanical and Aerospace Engineering and Institute of Advanced Machinery and Design, Seoul National University, Seoul 151-742, Korea. E-mail: sky4u@snu.ac.kr

<sup>b</sup>Harvard-MIT Division of Health Sciences and Technology, Brigham and Women's Hospital, Harvard Medical School, Boston, MA 02139, USA

† Electronic supplementary information (ESI) available: Photographs showing the stability of the PEG channels with different molecular weights using PEG-DA and PEG-DMA, and comparing the fabricated PEG microchips (on glass or PET film) with standard PDMS chip. See DOI: 10.1039/b610503c

## Methods and materials

### Fabrication of PEG micro/nanochannels

A small amount (50–200  $\mu\text{L}$ ) of UV curable low molecular weight (MW) PEG polymer such as PEG dimethacrylate (PEG-DMA, MW = 330, Aldrich) or PEG diacrylate (PEG-DA, MW = 258, Aldrich) were drop-dispensed on a silicon master and the supporting poly(ethylene terephthalate) (PET) film was carefully placed on top of the surface to make conformal contact.<sup>30</sup> The total thickness of PEG device ranged from  $\sim 100$  to  $\sim 250$   $\mu\text{m}$ , comprised of a 50  $\mu\text{m}$  PET film and 50–200  $\mu\text{m}$  PEG mold. The PET film used in this study was surface modified with urethane groups to increase adhesion to the acrylate-containing monomer (Minuta Tech. Korea). The silicon masters were prepared by photolithography and had protruding lines (ranging in diameter from 50 nm to 200  $\mu\text{m}$ ) or cylinders (30  $\mu\text{m}$  width and 12  $\mu\text{m}$  height), resulting in PEG replicas with the opposite sense. To cure, the sample was exposed to UV (250–400 nm) for a few seconds (PEG-DA) to a few tens of seconds (PEG-DMA) at an intensity of 90  $\text{mW cm}^{-2}$  after adding 1 wt% of the UV initiator (2,2-dimethoxy-2-phenylacetophenone, Aldrich) with respect to the amount of polymer. After UV curing, the fabricated PEG channel mold was peeled off from the master using a sharp tweezer. In the case of the glass cover slip, the surface was treated with an adhesion promoter (phosphoric acrylate or acrylic acid dissolved in propylene glycol monomethyl ether acetate (PGMEA), 10 vol%) to enhance the adhesion between the PEG and the substrate. The composite layer consisting of a replicated PEG mold and a supporting PET film was drilled to make inlet and outlet reservoirs and brought into contact with the PEG surface coated on a PET film or a glass slide. A slight physical pressure ( $\sim 10^3$  Pa) was applied to make conformal contact. With additional UV exposure for a few minutes, irreversible bonding occurred through photo-induced cross-linking at the interface.

### Fabrication of PDMS/unmodified glass and PDMS/PEG-coated glass microchannels

Microfluidic PDMS molds were fabricated by curing the prepolymer on silicon masters that had protruding features with the impression of microfluidic channels (ranging from 200 to 400  $\mu\text{m}$  in width with different heights). To cure the PDMS prepolymer, a mixture of 10 : 1 silicon elastomer and the curing agent was poured onto the master and placed at 70  $^{\circ}\text{C}$  for 2 h. The PDMS mold was then peeled from the silicon wafer and cut into narrow strips. For bonding PDMS channels, a microfluidic mold and a glass slide were plasma cleaned for 40 s (60s W, PDC-32G, Harrick Scientific, Ossining, NY). After plasma treatment, the microfluidic mold was brought in contact with the substrate and firmly pressed to form an irreversible seal. To fabricate PDMS channels on PEG-coated glass substrate, a PEG polymer was spin-coated on a narrow, exposed glass cover slip while covering the rest to be plasma cleaned with a thin scotch tape ( $\sim 10$   $\mu\text{m}$ ). After curing the PEG film and removing the scotch tape, the substrate was plasma cleaned while protecting the coated PEG layer with the same-sized PET film. The plasma cleaning

conditions were the same as those for PDMS channels on unmodified glass substrate. After plasma treatment, PDMS channels on PEG-coated glass were prepared using the same procedure.

### Scanning electron microscopy (SEM)

Images were taken using high-resolution SEM (S4800, Hitachi, Japan) at an acceleration voltage higher than 5 kV. Samples were coated with a 10 nm Au layer prior to analysis to prevent charging.

### Protein adsorption within microchannels

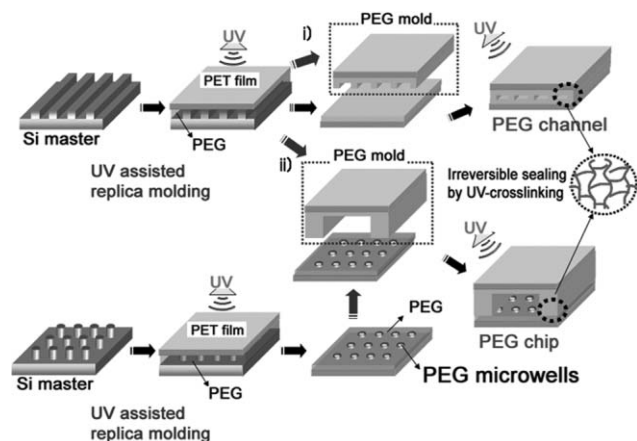
Fluorescein isothiocyanate labeled bovine serum albumin (FITC-BSA), fibronectin (FN), and goat anti-rabbit immunoglobulin G (FITC-IgG) were dissolved in PBS (pH = 7.4) at a concentration of 50  $\mu\text{g mL}^{-1}$ , 20  $\mu\text{g mL}^{-1}$  and 50  $\mu\text{g mL}^{-1}$ , respectively. To test for adhesion of protein within microfluidic channels, the primary protein was pumped through the microchannels for 30 min at a flow rate of 5  $\mu\text{L min}^{-1}$ . For FN staining, a solution of anti-FN antibody was flowed through the channel for an additional 45 min, followed by 1 h of FITC-labeled anti-rabbit secondary antibody. Then, the channels were rinsed thoroughly with PBS and subsequently analyzed using an inverted fluorescent microscope (Axiovert 200, Zeiss, 488 nm excitation and 530 nm detection). All protein-staining experiments were done in triplicate to ensure that multiple pictures were captured. Fluorescent images of various samples were taken and quantified using NIH-Scion Image viewer. Blank glass slides analyzed under the same light exposure were used as background controls.

### Cell adhesion within microchannels

NIH-3T3 murine embryonic fibroblasts were purchased from American Type Culture Collection (ATCC) and maintained in Dulbecco's Modified Eagle Medium (DMEM) supplemented with 10% fetal bovine serum (FBS) at 37  $^{\circ}\text{C}$  and 5%  $\text{CO}_2$  environment. For cell adhesion experiments, a solution of 20  $\mu\text{g mL}^{-1}$  of FN (Gibco Invitrogen Corporation, Carlsbad, CA) in PBS was flowed through the channel for 15 min followed by a suspension of cells ( $\sim 1\text{--}5 \times 10^7$  cells  $\text{mL}^{-1}$ ) in medium containing serum at a flow rate of 5  $\mu\text{L min}^{-1}$ . A detailed procedure for maintaining the cell culture system inside microchannels was reported previously.<sup>31</sup>

### Liposome preparation and labeling

The biotinylated lipid vesicles were kindly provided by Dr Hea Yeon Lee at Osaka University. Details on preparation and characterization of the vesicles were published elsewhere.<sup>32</sup> To generate micropatterns of supported lipid membrane inside the PEG channel, a solution of biotinylated lipid vesicles (labeled with fluorochrome DiI, 550 nm excitation and 565 nm detection) was flowed from the inlet reservoir through the patterned microfluidic channel (400  $\mu\text{m}$  width and 80  $\mu\text{m}$  height) at an initial velocity of  $\sim 170$   $\text{mm s}^{-1}$  using surface tension driven flow. For measuring biotin–streptavidin interactions, a solution of streptavidin (labeled with Alexa Fluor<sup>®</sup> 488, 495 nm excitation and 519 nm detection) dissolved in PBS



**Scheme 1** Schematic illustration of the experimental procedure. A flat or a patterned PEG substrate was used for the fabrication where (i) a flat PEG film led to simple channel arrays while (ii) a patterned substrate led to a PEG microchip with patterned microwells. Briefly, a few drops of a photocurable PEG monomer were drop-dispensed on a silicon master and molded by replica molding.<sup>33</sup> After exposure to UV light, the PEG mold was detached from the silicon master using a supporting PET film. For irreversible bonding in (i), a PEG film-coated glass or PET film was attached to the pre-defined PEG mold followed with UV exposure. Prior to the application of the PEG substrate, the PEG film was partially cured to prevent collapse or clogging of the channel.

(pH 7.4) at  $\sim 500 \mu\text{L min}^{-1}$  was run through the channel for 1 min. All patterned surfaces were then analyzed using an inverted fluorescent microscope (IX71, Olympus). All staining experiments were performed three to five times to ensure reliability of the data. Fluorescent images were taken and quantified using Image-pro plus 5.1 (Olympus).

## Results and discussion

### Fabrication of PEG micro- and nanochannels

The fabrication process is shown in Scheme 1. To determine the effect of PEG polymer properties on microchannel

fabrication, we tested the ability of acrylated PEG monomers with different molecular weights to form microchannels. It was found that a low molecular weight PEG dimethacrylate (PEG-DMA, MW = 330) or a PEG diacrylate (PEG-DA, MW = 258) resisted swelling in an aqueous solution for periods of up to 2 weeks. For high molecular weight polymers [e.g., PEG-DMA (MW = 770) and PEG-DA (MW = 875)], we observed significant swelling and collapse of the channels within 5 h of contact with water. This can be explained by the fact that a high molecular weight polymer renders a low crosslinking density, resulting in significant swelling.

During the fabrication of PEG channel mold, care was taken to retain the surface of the mold flat and incompletely cured. The flatness of the PEG mold was required to ensure conformal contact of the surfaces for bonding the mold to the substrate. In addition, the reactive, uncured acrylate groups of the mold facilitate photocrosslinking with the PEG coated glass or PET film, resulting in an irreversible seal without additional chemical/physical treatments. Also, the use of a supporting PET film to peel off the replicated PEG mold is essential since it can aid in releasing the mold from the silicon master and prevent swelling of the PEG layer. Without this supporting layer, an aqueous solution would continuously absorb and diffuse into the layer, resulting in destruction of the device. Compared to other methods such as plasma treatment, temperature annealing, or electric field-assisted bonding,<sup>33</sup> this bonding process is extremely simple and could be applied to many polymers containing UV curable groups.

An important parameter of this process is the curing time, which determines the ability of the molds to irreversibly bond to each other with good edge definition. If the curing time of PEG channel mold or PEG support layer is too long, no active groups would remain on the surface (bond failure). If the curing time is too short, on the other hand, the partially mobile PEG layer would fill into the void spaces, leading to clogging or collapse of the channel. To determine the optimal curing conditions, we tested various curing times on bonding between PEG mold and the PEG support layer using two different PEG polymers as shown in Fig. 1. A slight physical pressure ( $\sim 10^3$  Pa) was applied to make conformal contact. PEG-DA

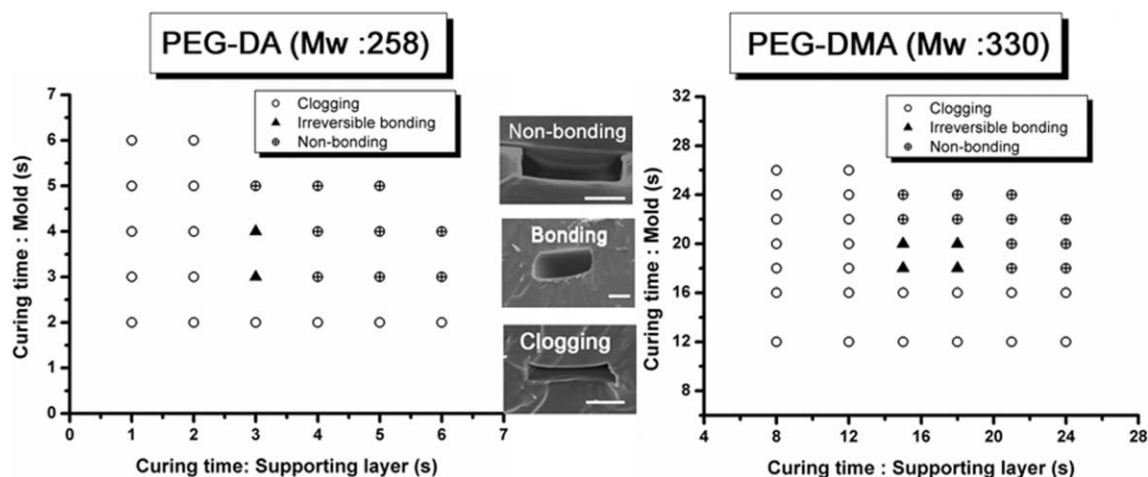


**Fig. 1** Diagrams for optimizing the mold and substrate bonding for PEG-DMA (MW = 330) and PEG-DA (MW = 258) under various curing times. To cure, the samples were exposed to UV ( $\lambda = 250\text{--}400$  nm) at an intensity of  $90 \text{ mW cm}^{-2}$ . The scale bar in the SEM images indicates  $5 \mu\text{m}$ .

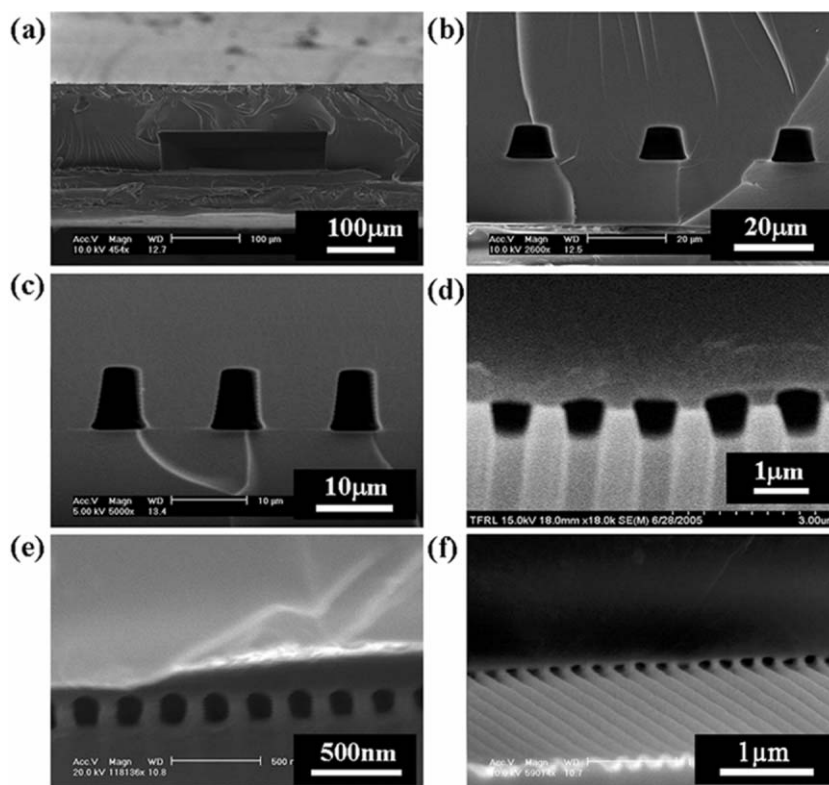


**Fig. 2** Cross-sectional SEM images of various PEG channels with size ranging from 200  $\mu\text{m}$  to 50 nm: (a) 200  $\mu\text{m}$  width, 80  $\mu\text{m}$  height, (b) 10  $\mu\text{m}$  width, 10  $\mu\text{m}$  height, (c) 8  $\mu\text{m}$  width, 10  $\mu\text{m}$  height, (d) 800 nm width, 1  $\mu\text{m}$  height, (e) 70 nm width, 100 nm height, and (f) 50 nm diameter.

cured faster than PEG-DMA and the presence of an optimal curing time for irreversible sealing of PEG mold and support layer was confirmed. For this experiment, we used microchannels of 10  $\mu\text{m}$  in width and 4  $\mu\text{m}$  in height but other channels showed similar results.

Fig. 2 shows the cross-sections of various PEG micro- and nanochannels using the irreversible bonding process. The channel size ranges from 200  $\mu\text{m}$  to 50 nm with different heights (Fig. 2(a)–(d)). As illustrated, the channels maintain sharp edges through the processing. In addition, two surfaces were completely sealed since the interface between the mold and the film was hardly visible. For nanochannels that were less than  $\sim 100$  nm in diameter, a slight rounding of the PEG channel mold was observed, which in turn produced rounded corners as shown in Fig. 2(e)–(f). Nonetheless, the overall shapes did not strongly deviate from the original silicon masters that were rectangular in shape (data not shown). For nanochannels, channels with low aspect ratios were prone to clogging. Since the elastic modulus of the crosslinked PEG material was measured to be  $\sim 1$  GPa, it appears that clogging takes place by partial filling of the mobile PEG film into the cavity of the PEG mold. Therefore, the degree of crosslinking needs to be maintained at the optimum level as demonstrated in Fig. 1.

#### Protein adsorption and cell adhesion inside PEG microchannels

To assess the non-biofouling nature of PEG microchannel, FITC-BSA, FN, and FITC-IgG were flowed through three types of 200  $\mu\text{m}$  channels (PDMS/glass, PDMS/PEG-coated

glass, and PEG channels/unmodified glass) for 5 h, respectively. Experiments demonstrated that the adsorption of BSA, FN, and IgG (5.6%, 1.2%, 0.1% adsorption relative to BSA on glass, respectively) was significantly reduced on PEG channels compared to the other channels (Fig. 3a). These results indicate that the PEG microchannels are intrinsically resistant to fouling.

To minimize swelling, we used low molecular weight PEG-DMA (MW = 330) and 1% photoinitiator.<sup>34</sup> We have observed that higher molecular weight PEG polymers were significantly more prone to swelling, leading to channel blockage and delamination of the PEG mold from the substrate. In contrast, channels that were made from low molecular weight PEG polymers showed excellent stability. The stability of the device is closely related to the adhesion at the PEG mold to the supporting substrate (glass cover slip or PET film) interface. It was found that a PEG layer adhered firmly to a PET film due to the presence of polyurethane groups on the modified PET surface and thus no additional treatment was needed. This may be attributed to hydrogen bonding and polar interactions at the interface. On the other hand, glass surfaces had to be treated with an adhesion promoter that has an anchoring group with hydrophilic moieties on glass surface and another anchoring group with an acrylate monomer (see experimental protocol). This simple bonding process offers an innovative way of solving swelling problems in PEG-based channels by introducing a supporting substrate with strong interactions with the PEG hydrogel.

We also tested for the ability of PEG channels to prevent cell adhesion. It was found that fewer NIH-3T3 murine embryonic

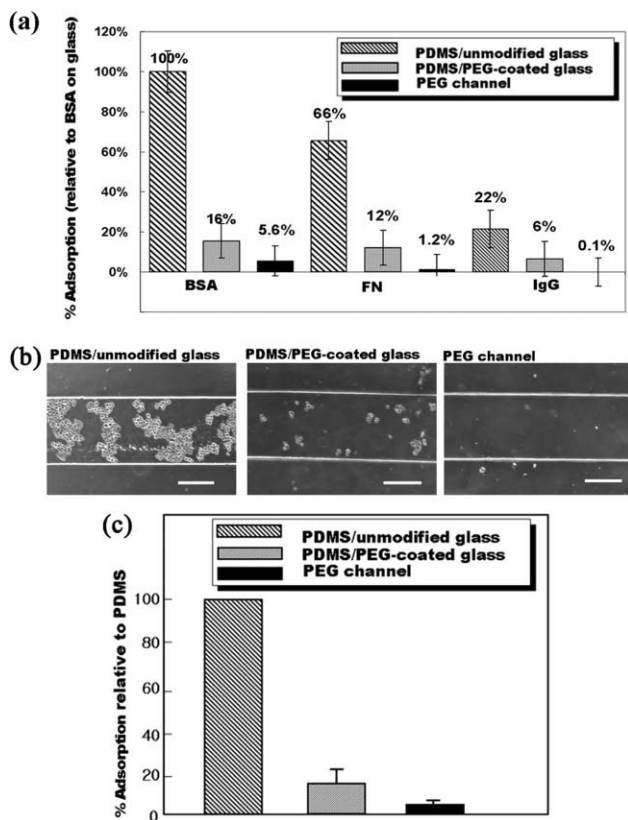


**Fig. 3** (a) A quantitative analysis of the fluorescent images for protein adsorption where BSA, FN, and IgG were flowed inside three types of 200  $\mu\text{m}$  channels with 80  $\mu\text{m}$  height (PDMS/glass, PDMS/PEG-coated glass, and PEG channels/unmodified glass, respectively). (b) Optical micrographs for the adhesion of NIH-3T3 murine embryonic fibroblasts using the same channels. (c) A quantitative analysis indicates that the PEG channels were the most resistant against cell adhesion ( $< \sim 2\%$  compared to the PDMS channel).

fibroblasts adhered to PEG channels in comparison to controls (PDMS channel on unmodified glass or on PEG-coated glass) as shown in Fig. 3(b)–(c). To analyze cell adhesion within the microchannels, cells were seeded within the channels for 6 h and subsequently washed and the degree of cell adhesion was analyzed under an optical microscope. For cell adhesion, each channel was pre-treated with FN for 15 min prior to cell seeding, since FN is an extracellular matrix protein to promote cell adsorption.<sup>35</sup> As shown in Fig. 3(b), cell adhesion was greatly reduced inside PEG channel compared to the unmodified PDMS channel. Although cell adhesion was reduced inside PDMS channels on PEG-coated glass ( $< \sim 20\%$  with respect to the unmodified PDMS channel), the PEG molded channels were the most resistant ( $< \sim 2\%$  with respect to the unmodified PDMS channel) (Fig. 3(c)). Furthermore, adhered cells were usually isolated with rounded morphology inside the PEG channel, suggesting that their adhesion was weak.

#### Biotin–streptavidin bindings inside PEG microchannels

Recently, we demonstrated that well-defined microarrays of supported lipid bilayers (SLBs) could be generated inside a PDMS channel by combining non-biofouling PEG

microwells.<sup>36</sup> To further improve the lipid-based microfluidic device for analytical applications, monolithic PEG microchannels were fabricated with PEG microwells located inside the bottom of the channel as shown in Scheme 1 and Fig. 4(a) and (b). The patterned arrays of SLBs were used to test biotin–streptavidin chemistry. First, biotinylated lipid vesicles were flowed through the patterned microfluidic channel by surface tension driven filling since the PEG channels are intrinsically hydrophilic (contact angle of water  $\sim 30^\circ$ ). As reported earlier,<sup>36</sup> the lipid bilayer membranes were formed by fusion of patterned lipid vesicles onto exposed, hydrophilic glass substrate. Subsequently, biotin–streptavidin bindings were measured under a fluorescence microscope by flowing Alexa 488-conjugated streptavidin as a receptor. The lipid bilayer membranes were neatly patterned onto the pre-defined regions of the substrate (Fig. 4(c) and (d)). Non-specific adsorption, which is frequently observed for most microfluidic devices, was not seen. Also, streptavidin was selectively deposited with the biotinylated lipid bilayer membrane (Fig. 4(e)–(f)), suggesting that the current device could act as a lipid-based bioassay-chip or biosensor using antigen–antibody interactions.

#### Conclusions

We have presented a simple, yet robust method for fabricating PEG-based micro- and nano-channels using an acrylate-containing monomer such as PEG-DMA or PEG-DA by UV-assisted bonding. Using this strategy, a non-biofouling, flexible polymer microfluidic device was fabricated without surface modification. Although there have been a number of approaches to render microfluidic channels non-biofouling, additional modification always results in less reliability and

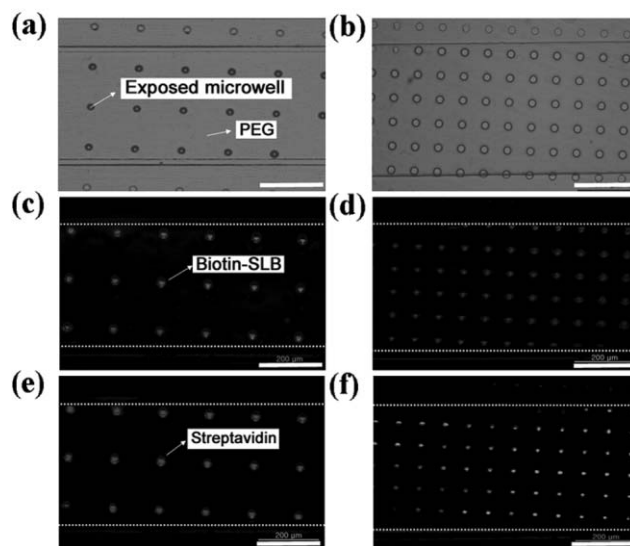


**Fig. 4** (a), (b) Optical micrographs of the PEG channels (400  $\mu\text{m}$  width, 80  $\mu\text{m}$  height) combined with PEG microwells (30  $\mu\text{m}$  width, 12  $\mu\text{m}$  height) of two different densities (180  $\mu\text{m}$  and 60  $\mu\text{m}$  center-to-center distance for (a) and (b), respectively). (c), (d) Fluorescent images of the patterned biotinylated lipid membranes after selective deposition onto the exposed regions. (e), (f) Fluorescent images of the same regions in (b), (c) after conjugation with Alexa Fluor<sup>®</sup> 488 streptavidin. The scale bar is 200  $\mu\text{m}$ .

more complexity. In our study, we attempted to offer a generic way of addressing this problem in a simple and economical fashion. The total time it takes to fabricate a channel including replica molding and UV-assisted bonding is less than 30 min, dramatically enhancing the practical usefulness. Furthermore, the PEG channels showed excellent resistant properties against protein adsorption ( $< \sim 5\%$ ) and cell adhesion ( $< \sim 2\%$ ) with respect to PDMS channel without additional modification of the channel. A simple device based on lipid-based affinity binding was also fabricated using a PEG channel with patterned PEG microwells. It was found that the biotin-streptavidin interactions could be easily included and tested inside the PEG channel in a pumpless scheme without biofouling. It is envisioned that the PEG-based microfluidic system developed here could be an improved method of fabricating bioanalytical and biomedical microdevices.

## Acknowledgements

This research was supported by the Korean Research Foundation Grant funded by the Korean Government (MOEHRD) (KRF-2005-041-D00111) and the Micro Thermal System Research Center of Seoul National University, and the Seoul R&BD Program (Seoul Research and Business Development Program). The authors would like to thank Judy Yeh for technical support and Dr Hea Yeon Lee for providing biotinylated lipid vesicles.

## References

- 1 A. Y. Fu, C. Spence, A. Scherer, F. H. Arnold and S. R. Quake, *Nat. Biotechnol.*, 1999, **17**, 1109–1111.
- 2 M. A. Burns, B. N. Johnson, S. N. Brahmaandra, K. Handique, J. R. Webster, M. Krishnan, T. S. Sammarco, P. M. Man, D. Jones, D. Heldsinger, C. H. Mastrangelo and D. T. Burke, *Science*, 1998, **282**, 484–487.
- 3 A. Bernard, D. Fitzli, P. Sonderegger, E. Delamarche, B. Michel, H. R. Bosshard and H. Biebuyck, *Nat. Biotechnol.*, 2001, **19**, 866–869.
- 4 D. T. Chiu, N. L. Jeon, S. Huang, R. S. Kane, C. J. Wargo, I. S. Choi, D. E. Ingber and G. M. Whitesides, *Proc. Natl. Acad. Sci. U. S. A.*, 2000, **97**, 2408–2413.
- 5 D. J. Beebe, J. S. Moore, J. M. Bauer, Q. Yu, R. H. Liu, C. Devadoss and B. H. Jo, *Nature*, 2000, **404**, 588–590.
- 6 E. Delamarche, D. Juncker and H. Schmid, *Adv. Mater.*, 2005, **17**, 2911–2933.
- 7 D. J. Harrison, A. Manz, Z. H. Fan, H. Luedi and H. M. Widmer, *Anal. Chem.*, 1992, **64**, 1926–1932.
- 8 J. N. Turner, W. Shain, D. H. Szarowski, M. Andersen, S. Martins, M. Isaacson and H. Craighead, *Exp. Neurol.*, 1999, **156**, 33–49.
- 9 T. J. Johnson, D. Ross, M. Gaitan and L. E. Locascio, *Anal. Chem.*, 2001, **73**, 3656–3661.
- 10 D. C. Duffy, J. C. McDonald, O. J. A. Schueller and G. M. Whitesides, *Anal. Chem.*, 1998, **70**, 4974–4984.
- 11 G. Ocvirk, M. Munroe, T. Tang, R. Oleschuk, K. Westra and D. J. Harrison, *Electrophoresis*, 2000, **21**, 107–115.
- 12 D. Gingell, N. Owens, P. Hodge, C. V. Nicholas and R. Odell, *J. Biomed. Mater. Res.*, 1994, **28**, 505–513.
- 13 M. B. Stark and K. Hlmgberg, *Biotechnol. Bioeng.*, 1989, **34**, 942–950.
- 14 M. Malmsten, K. Emoto and J. M. Van Alstine, *J. Colloid Interface Sci.*, 1998, **202**, 507–517.
- 15 K. C. Popat, R. W. Johnson and T. A. Desai, *J. Vac. Sci. Technol., B*, 2003, **21**, 645–654.
- 16 K. C. Popat and T. A. Desai, *Biosens. Bioelectron.*, 2004, **19**, 1037–1044.
- 17 J. Lahann, M. Balcells, H. Lu, T. Rodon, K. F. Jensen and R. Langer, *Anal. Chem.*, 2003, **75**, 2117–2122.
- 18 M. Q. Zhang, T. Desai and M. Ferrari, *Biomaterials*, 1998, **19**, 953–960.
- 19 V. Linder, E. Verpoorte, W. Thormann, N. F. de Rooij and M. Sigrist, *Anal. Chem.*, 2001, **73**, 4181–4189.
- 20 J. P. Rolland, R. M. Van Dam, D. A. Schorzman, S. R. Quake and J. M. DeSimone, *J. Am. Chem. Soc.*, 2004, **126**, 2322–2323.
- 21 K. R. King, C. C. J. Wang, M. R. Kaazempur-Mofrad, J. P. Vacanti and J. T. Borenstein, *Adv. Mater.*, 2004, **16**, 2007–2012.
- 22 R. P. Sebra, K. S. Anseth and C. N. Bowman, *J. Polym. Sci., Part A: Polym. Chem.*, 2006, **44**, 1404–1413.
- 23 K. T. Haraldsson, J. B. Hutchison, R. P. Sebra, B. T. Good, K. S. Anseth and C. N. Bowman, *Sens. Actuators, B*, 2006, **113**, 454–460.
- 24 J. Kobayashi, M. Yamato, K. Itoga, A. Kikuchi and T. Okano, *Adv. Mater.*, 2004, **16**, 1997–2001.
- 25 A. Paguirigan and D. J. Beebe, *Lab Chip*, 2006, **6**, 407–413.
- 26 G. S. Fiorini and D. T. Chiu, *Biotechniques*, 2005, **38**, 429–446.
- 27 J. Atencia and D. J. Beebe, *Nature*, 2005, **437**, 648–655.
- 28 J. B. Hutchison, K. T. Haraldsson, B. T. Good, R. P. Sebra, N. Luo, K. S. Anseth and C. N. Bowman, *Lab Chip*, 2004, **4**, 658–662.
- 29 D. J. Beebe, J. S. Moore, Q. Yu, R. H. Liu, M. L. Kraft, B. H. Jo and C. Devadoss, *Proc. Natl. Acad. Sci. U. S. A.*, 2000, **97**, 13488–13493.
- 30 S. J. Choi, P. J. Yoo, S. J. Baek, T. W. Kim and H. H. Lee, *J. Am. Chem. Soc.*, 2004, **126**, 7744–7745.
- 31 A. Khademhosseini, K. Y. Suh, S. Jon, G. Eng, J. Yeh, G. J. Chen and R. Langer, *Anal. Chem.*, 2004, **76**, 3675–3681.
- 32 R. C. M. R. I. MacDonald, B. P. Menco, K. Takeshita, N. K. Subbarao and L. R. Hu, *Biochim. Biophys. Acta*, 1991, **1061**, 297–303.
- 33 D. Mijatovic, J. C. T. Eijkel and A. van den Berg, *Lab Chip*, 2005, **5**, 492–500.
- 34 L. M. Schwarte and N. A. Peppas, *Polymer*, 1998, **39**, 6057–6066.
- 35 E. Ostuni, R. Kane, C. S. Chen, D. E. Ingber and G. M. Whitesides, *Langmuir*, 2000, **16**, 7811–7819.
- 36 P. Kim, S. E. Lee, H. S. Jung, H. Y. Lee, T. Kawai and K. Y. Suh, *Lab Chip*, 2006, **6**, 54–59.